Title
COMMENTS ON Y polarized ---> ""* &

Authors
Beder, Douglas S.
Soding, Paul.

Publication Date
1967-08-10

UCRL-17867
c. 2

University of California

Ernest O. Lawrence Radiation Laboratory

COMMENTS ON $\gamma_{polarized}$ N → $\pi\Delta$

Douglas S. Beder and Paul Söding

August 10, 1967

DISCLAIMER

UCRL-17867
UC-34 Physics
TID-4500 (50th Ed.)

UNIVERSITY OF CALIFORNIA
Lawrence Radiation Laboratory
Berkeley, California

AEC Contract No. W-7405-eng-48

COMMENTS ON $\gamma_{\text{polarized}} N \rightarrow \pi \Delta$

Douglas S. Beder and Paul Söding

August 10, 1967

Printed in the United States of America
Available from
Clearinghouse for Federal Scientific and Technical Information
National Bureau of Standards, U.S. Department of Commerce
Springfield, Virginia 22151
Price: Printed Copy $3.00; Microfiche $0.65

COMMENTS ON $\gamma_{\text{polarized}} N \rightarrow \pi\Delta$

Douglas S. Beder* and Paul Söding

Lawrence Radiation Laboratory
University of California
Berkeley, California

August 10, 1967

ABSTRACT

Expressions are given for the production and decay angular correlations in the reaction $\gamma p \rightarrow \pi\Delta$ [with $J^P(\Delta) = 3/2^+$] with polarized photons. The use of this reaction to determine properties of s-channel baryonic resonances is discussed. The results are illustrated by examples showing which information can be obtained, in particular in the 1450-MeV and 1680-MeV resonance regions, with polarized (or unpolarized) photon beams.

I. INTRODUCTION

This note presents some comments on the use of polarized photon beams to study a particular reaction,[1] namely $\gamma N \rightarrow \pi\Delta$ (1236 MeV). We shall restrict our considerations to the "low" energy region, where s-channel baryon resonances are prominent, and will therefore mainly utilize this reaction to obtain information about these (intermediate state) resonances. For this purpose, the reaction under consideration has certain advantages, compared with $\gamma N \rightarrow \pi N$, say, because of the additional information afforded by observing the Δ decay distributions, and also because of the rather large cross sections involved ($\sigma \approx 70$ μb at $E_{c.m.} \approx 1400$ MeV).

The properties of the baryon resonances are of two types:

(i) J^P, independent of electromagnetism;

(ii) Characteristics of the electromagnetic excitation process.

We shall assume that both circularly polarized (i.e., definite helicity) and linearly polarized γ's will be available (as would certainly be the case for a γ beam produced by backscattering laser light off an electron beam[2]). The merits of either polarization will be considered in relation to information of types (i) and (ii). In Sec. II we present general formalism, followed by a more detailed example illustrating "baryon spectroscopy" in Sec. III. In Sec. IV we comment on models of the reaction, in particular on one-pion exchange. Finally, in Sec. V we illustrate how baryon resonance properties are exhibited in the (production) angle dependence of the measured density matrix elements.

II. GENERAL FORMALISM

We first define our coordinate systems (see Fig. 1). The momentum of the photon in the c.m. specifies the positive z direction. The production reaction is defined to occur in the xz plane of the c.m. system; if the γ is linearly polarized, its polarization vector $\vec{\epsilon}$ can be inclined at (azimuthal) angle Φ to the xz plane. The decay distributions of the Δ are conveniently examined in the rest frame of the Δ, with the $\bar{z}$ axis of this frame parallel to the direction of the Δ three-momentum in the c.m. The $\bar{y}$ axis of this rest frame is the same as the y-axis of the c.m. frame.

The Δ rest frame so defined differs from the Gottfried-Jackson[3] rest frame only by a rotation about the y axis. Our motivation for the present

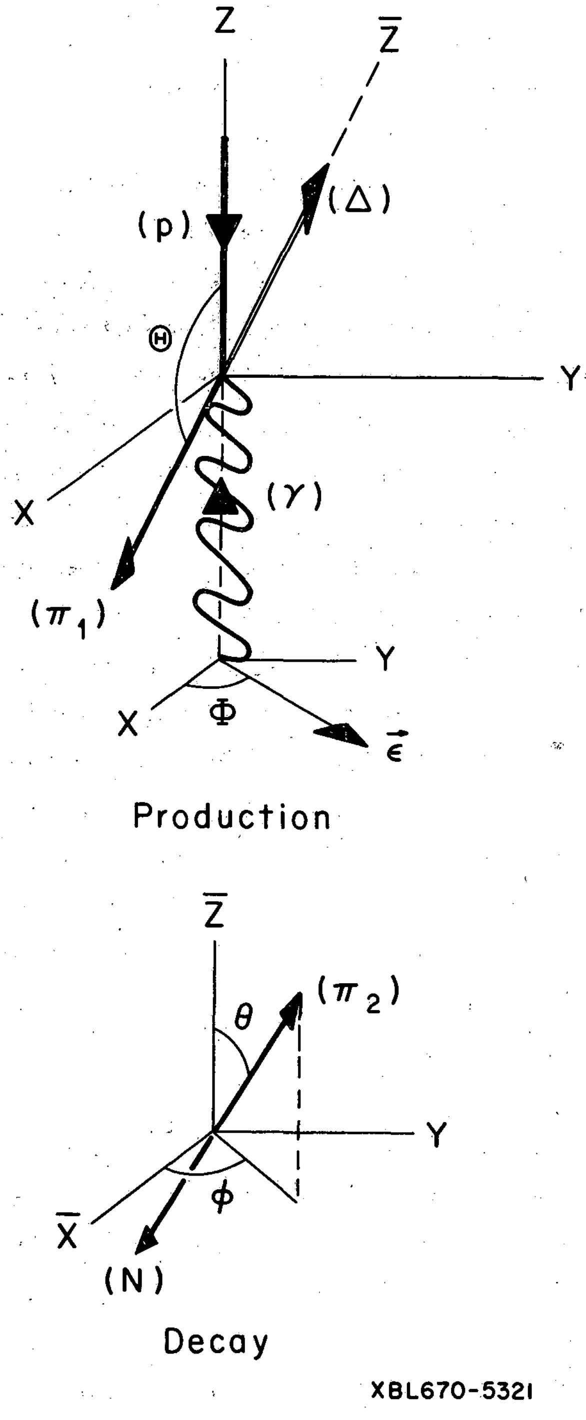

Fig. 1. Coordinate systems used to describe production and decay of the Δ.

choice is that the Δ helicity in the c.m. frame is the same as the rest frame (ours) $J_{\bar{z}}$ of the Δ. The angular distributions in our rest frame are therefore conveniently specified by the production density matrix in a helicity basis[4] in the c.m. frame. This feature is appropriate, since we wish to study properties of s-channel (intermediate) resonances.

In the c.m. frame we denote the production amplitude by $T_\Lambda^{(\lambda)}$, where λ is the photon helicity and Λ the helicity of the Δ, and we suppress nucleon helicity indices and the production polar angle Θ. Similarly the Δ decay amplitude in its rest frame is denoted by $A_\Lambda(\theta,\phi)(\Lambda = -3/2, \cdots, +3/2)$, where (θ,ϕ) are the decay pion angles in the Δ rest frame, and where we again suppress the final nucleon helicity label. Let Ω be the production solid angle.

The distribution of the decay pion (π_2) is then given by

$$\frac{d\sigma\,(\lambda;\theta\phi)}{d\Omega\, d\cos\theta\, d\phi} = \frac{q_\pi}{64\,\pi^2 s k_\gamma} \left| \sum_\Lambda T_\Lambda^{(\lambda)}\, A_\Lambda(\theta,\phi) \right|^2, \tag{1}$$

where s is the c.m. energy squared, and k_γ and q_π are the c.m. momenta of the incident photon and outgoing pion π_1, respectively. Here we imply summation over all nucleon spins. The Σ factor in Eq. 1 can be written as

$$\left|\sum\right|^2 \equiv \mathrm{Tr}\,(\rho^{(\lambda)}\, D) \tag{2}$$

where

$$\rho_{\Lambda\Lambda'}^{(\lambda)} \equiv T_\Lambda^{(\lambda)}\, T_{\Lambda'}^{*(\lambda)}, \quad \text{summed over incident nucleon spins}$$

$$D_{\Lambda\Lambda'} \equiv A_\Lambda^*\, A_{\Lambda'}, \quad \text{summed over decay nucleon spins} \tag{3}$$

$(\rho^{(\lambda)}$ is just an unnormalized density matrix).

If we normalize $\sum_{\substack{\text{(helicity of}\\ \text{decay nucleon)}}} \int d\omega\, |A_\Lambda|^2 = 1$, then the production differential cross section for a Δ with definite helicity Λ is just

$$\frac{d\sigma(\lambda;\Lambda)}{d\Omega} = \frac{q_\pi}{64\pi^2 s\, k_\gamma} \left| T_\Lambda^{(\lambda)} \right|^2 \tag{4}$$

in the c.m. system. We have written $d\omega = d\cos\theta\, d\phi$.

The partial-wave expansion for $T^{(\lambda)}_{\Lambda\mu}$ is well known[4] (we now need to exhibit the initial-state nucleon helicity μ):

$$T^{(\lambda)}_{\Lambda\mu}(\Theta) = \sum_J (2J+1)\langle\Lambda|T^J|\lambda\mu\rangle\, d^J_{\lambda-\mu,-\Lambda}(\Theta). \tag{5}$$

For a definite spin parity J^P transition (e.g., via an intermediate definite parity resonance), an important property is[4]

$$\langle\Lambda|T^J|\lambda\mu\rangle = P(-)^{J-1/2}\langle-\Lambda|T^J|\lambda\mu\rangle \equiv \alpha\langle-\Lambda|T^J|\lambda\mu\rangle, \text{ say.} \tag{6}$$

Therefore, to determine the parity of a resonance, one can simply make a comparison of $\rho^{(\lambda)}_{\Lambda,\Lambda'}$ and $\rho^{(\lambda)}_{\Lambda,-\Lambda'}$, and extract the phase α. We shall illustrate this in the next section.

We next proceed to obtain more explicit expressions for the quantities of Eq. 3.

Defining $A_\Lambda(\theta,\phi) = C(L\ 1/2\ S;\ \Lambda-\nu,\nu)\, Y_L^{\Lambda-\nu}(\theta,\phi)$ to be the decay amplitude for $\Delta(P\text{ wave }\pi N)\to\pi+N$, where ν is the spin component of the N in $\overline{z}$ direction (note that $\sum_\nu\int|A_{\Lambda(\nu)}|^2\,d\omega = 1$), we obtain[5]

$$D_{\Lambda\Lambda'} = \sum_{K\text{ even}} (2L+1)\sqrt{\frac{2S+1}{4\pi}}\,(-)^{S-1/2}\, C(LLK;00)\, C(SKS;-\Lambda,\Lambda-\Lambda') \times W(SSLL;K\ 1/2)\, Y^K_{\Lambda'-\Lambda}(\theta,\phi). \tag{7}$$

Here we will have $L = 1$, $S = 3/2$. This has the general property $D_{\Lambda,-\Lambda} = 0$, and hence we cannot obtain $\rho^{(\lambda)}_{\Lambda,-\Lambda}$ from decay angular distributions alone.

Leaving out inconvenient normalizations, we then obtain for our case

$$D_{\Lambda\Lambda'} \propto \begin{array}{c|cccc} & 3 & 1 & -1 & -3 \\ \hline 3 & \sin^2\theta & -\frac{1}{\sqrt3}e^{-i\phi}\sin 2\theta & -\frac{1}{\sqrt3}e^{-2i\phi}\sin^2\theta & 0 \\ 1 & -\frac{1}{\sqrt3}e^{i\phi}\sin2\theta & \frac13+\cos^2\theta & 0 & -\frac{1}{\sqrt3}e^{-2i\phi}\sin^2\theta \\ -1 & -\frac{1}{\sqrt3}e^{2i\phi}\sin^2\theta & 0 & \frac13+\cos^2\theta & +\frac{1}{\sqrt3}e^{-i\phi}\sin2\theta \\ -3 & 0 & -\frac{1}{\sqrt3}e^{2i\phi}\sin^2\theta & +\frac{1}{\sqrt3}e^{i\phi}\sin2\theta & \sin^2\theta \end{array}. \tag{8}$$

The density matrix $\rho^{(\lambda)}$ has fewer symmetry properties than one is accustomed to, because of the fixed photon helicity. We define the density matrix elements by

$$\rho^{(+1)}_{\Lambda\Lambda'} = \begin{pmatrix} \rho_{33} & \rho_{31} & \rho_{3-1} & \rho_{3-3} \\ \rho^*_{31} & \rho_{11} & \rho_{1-1} & \rho^*_{-3\,1} \\ \rho^*_{3-1} & \rho^*_{1-1} & \rho_{-1-1} & \rho^*_{-3\,-1} \\ \rho^*_{3-3} & \rho_{-3\,1} & \rho_{-3-1} & \rho_{-3-3} \end{pmatrix} \tag{9}$$

It is easily shown that

$$\rho^{(-1)}_{\Lambda,\Lambda'} = (-)^{\Lambda-\Lambda'}\,\rho^{(+1)}_{-\Lambda,-\Lambda'} \, . \tag{10}$$

From this we directly obtain the decay angular distributions:

$$\begin{aligned} d\sigma\,(\pm 1;\theta,\phi) \;\propto\; & \\ & \frac{1}{2}\,(\rho_{33}+\rho_{-3-3})\sin^2\theta + \frac{1}{2}\,(\rho_{11}+\rho_{-1-1})(\frac{1}{3}+\cos^2\theta) \\ & -\frac{1}{\sqrt{3}}\,\mathrm{Re}\,[(\rho_{31}-\rho^*_{-3-1})\,e^{\pm i\phi}]\sin 2\theta \\ & -\frac{1}{\sqrt{3}}\,\mathrm{Re}[(\rho_{3-1}+\rho^*_{-3+1})\,e^{\pm 2i\phi}]\sin^2\theta \\ & = \frac{1}{2}\,(\rho_{33}+\rho_{-3-3})\sin^2\theta + \frac{1}{2}\,(\rho_{11}+\rho_{-1-1})(\frac{1}{3}+\cos^2\theta) \\ & -\frac{1}{\sqrt{3}}\,\mathrm{Re}(\rho_{31}-\rho_{-3-1})\sin 2\theta\cos\phi \pm \frac{1}{\sqrt{3}}\,\mathrm{Im}\,(\rho_{31}+\rho_{-3-1})\sin 2\theta\sin\phi \\ & -\frac{1}{\sqrt{3}}\,\mathrm{Re}(\rho_{3-1}+\rho_{-31})\sin^2\theta\cos 2\phi \pm \frac{1}{\sqrt{3}}\,\mathrm{Im}\,(\rho_{3-1}-\rho_{-31})\sin^2\theta\sin 2\phi \, . \end{aligned} \tag{11}$$

We notice that $d\sigma(\pm 1;\theta,\phi)$ differ only by terms in $\sin n\phi$, involving ρ_{31}, ρ_{3-1} which we earlier indicated to be relevant to obtaining parity information. Furthermore, since these terms are imaginary parts of ρ, only interferences between different phase amplitudes (e.g., different resonances) contribute. Notice that even the "unpolarized" angular distributions contain enough information to furnish all the measurable real parts of density matrix elements. Working with circularly polarized photons, one can select the two terms containing Imρ out of $d\sigma$ by taking the difference $d\sigma(\lambda=+1) - d\sigma(\lambda=-1)$. This may reduce the background and make the analysis simpler.

For linearly polarized photons, with the polarization making an angle Φ with the production plane,

$$\vec{\epsilon} \equiv \cos\Phi\, \vec{\epsilon}_x + \sin\Phi\, \vec{\epsilon}_y , \tag{12}$$

we find that the density matrix is

$$\rho^L(\Phi) = \frac{1}{2}\left(\rho^{(+1)} + \rho^{(-1)}\right) + \cos 2\Phi\, \rho^{(a)} + \sin 2\Phi\, \rho^{(b)}, \tag{13}$$

where

$$\rho^{(a)}_{\Lambda\Lambda'} = -\frac{1}{2}\left(T^{(+)}_{\Lambda} T^{*(-)}_{\Lambda'} + T^{(-)}_{\Lambda} T^{*(+)}_{\Lambda'}\right),$$
$$\rho^{(b)}_{\Lambda\Lambda'} = -\frac{i}{2}\left(T^{(+)}_{\Lambda} T^{*(-)}_{\Lambda'} - T^{(-)}_{\Lambda} T^{*(+)}_{\Lambda'}\right). \tag{14}$$

Thus, $\Phi = 0$ deg, 90 deg involves only $\rho^{(+)}$, $\rho^{(-)}$, and $\rho^{(a)}$, while $\rho^{(b)}$ describes the difference between the distributions for $\Phi = 45$ deg and $\Phi = 135$ deg. Note that

$$\rho^{(a)}_{-\Lambda,-\Lambda'} = (-)^{\Lambda-\Lambda'}\, \rho^{(a)}_{\Lambda\Lambda'}$$

and (15)

$$\rho^{(b)}_{-\Lambda,-\Lambda'} = -(-)^{\Lambda-\Lambda'}\, \rho^{(b)}_{\Lambda\Lambda'} .$$

Furthermore, in the decay angular distribution (11), $\rho^{(a)}$ contributes only to $(\rho^L_{33} + \rho^L_{-3-3})$, $(\rho^L_{11} + \rho^L_{-1-1})$, Re$(\rho^L_{31} - \rho^L_{-3-1})$, and Re$(\rho^L_{3-1} + \rho^L_{-31})$, and $\rho^{(b)}$ contributes only to Im$(\rho^L_{31} + \rho^L_{-3-1})$and Im$(\rho^L_{3-1} - \rho^L_{-31})$. This is intuitively clear, since for $\phi = 0$ deg, 90 deg, parity conservation excludes terms in (11) that change sign under $\phi \to 2\pi - \phi$, whereas the difference of the distributions for $\Phi = 45$ deg and $\Phi = 135$ deg must be odd under $\phi \to 2\pi - \phi$.

III. EXTRACTION OF RESONANCE PARAMETERS

In this section we illustrate the types of measurements needed to obtain resonance properties; we use a simple example where only one definite parity resonance is present. For this case (taking $\lambda = +1$ implicitly), ρ is real; some of the useful ρ's are exhibited below.

$$\left(\frac{1}{2J+1}\right)^2 \mathrm{Re}(\rho_{31} - \rho_{-3-1}) = \mathrm{Re}\langle \tfrac{3}{2}||\tfrac{3}{2}\rangle \langle \tfrac{1}{2}||\tfrac{3}{2}\rangle^* (d^J_{3/2-3/2}\, d^J_{3/2-1/2} - d^J_{3/2+3/2}\, d^J_{3/2+1/2}) + \mathrm{Re}\langle \tfrac{3}{2}||\tfrac{1}{2}\rangle \langle \tfrac{1}{2}||\tfrac{1}{2}\rangle^* (d^J_{1/2-3/2}\, d^J_{1/2-1/2} - d^J_{1/2+3/2}\, d^J_{1/2+1/2}) \tag{16a}$$

$$\left(\frac{1}{2J+1}\right)^2 \mathrm{Re}(\rho_{3-1} + \rho_{-3+1}) = \alpha\, \mathrm{Re}\langle \tfrac{3}{2}||\tfrac{3}{2}\rangle \langle \tfrac{1}{2}||\tfrac{3}{2}\rangle^* (d^J_{3/2-3/2}\, d^J_{3/2+1/2} + d^J_{3/2+3/2}\, d^J_{3/2-1/2}) + \alpha\, \mathrm{Re}\langle \tfrac{3}{2}||\tfrac{1}{2}\rangle \langle \tfrac{1}{2}||\tfrac{1}{2}\rangle^* (d^J_{1/2-3/2}\, d^J_{1/2+1/2} + d^J_{1/2+3/2}\, d^J_{1/2-1/2}) \tag{16b}$$

$$\left(\frac{1}{2J+1}\right)^2 (\rho_{33} + \rho_{-3-3}) = |\langle \tfrac{3}{2}||\tfrac{3}{2}\rangle|^2 \left((d^J_{3/2-3/2})^2 + (d^J_{3/2+3/2})^2\right) + |\langle \tfrac{3}{2}||\tfrac{1}{2}\rangle|^2 \left((d^J_{1/2-3/2})^2 + (d^J_{1/2+3/2})^2\right) \tag{16c}$$

$$-2\left(\frac{1}{2J+1}\right)^2 \rho^{(a)}_{33} = \alpha \langle \tfrac{3}{2}||\tfrac{3}{2}\rangle \langle \tfrac{3}{2}||\tfrac{1}{2}\rangle^* d^J_{3/2-3/2}\, d^J_{-1/2-3/2} + \alpha \langle \tfrac{3}{2}||\tfrac{1}{2}\rangle \langle \tfrac{3}{2}||\tfrac{3}{2}\rangle^* d^J_{1/2-3/2}\, d^J_{-3/2-3/2} + \text{etc.} \tag{16d}$$

The argument of the d's is Θ, the production polar angle.

To obtain the parity via phase α, we need (16a) and (16b) at two different values of Θ, so as to separate out terms from initial total helicity 3/2 and 1/2. If linearly polarized γ's are used, there would be a $\rho^{(a)}_{31}$ term, which could be untangled from ρ_{31} only if measurements are made at further values of Θ. We thus see that for determining parity it is advantageous to use circularly polarized photons.

On the other hand, from (16c) (and the analogous expressions for ρ_{11}), which is obtained even from the unpolarized reaction, one can obtain

$$|\langle \tfrac{3}{2}||\tfrac{3}{2}\rangle| \text{ and } |\langle \tfrac{3}{2}||\tfrac{1}{2}\rangle| \text{ (as well as } |\langle \tfrac{1}{2}||\tfrac{3}{2}\rangle| \text{ and } |\langle \tfrac{1}{2}||\tfrac{1}{2}\rangle|$$

from ρ_{11}). Again, these two amplitudes, representing transitions to the same final state (strongly interacting), should be relatively real for a given resonance. To obtain their relative sign, however, one has to make a linear polarization measurement, such as

$$\rho_{33}^{(a)} \sim \left|\langle \tfrac{3}{2} || \tfrac{3}{2} \rangle\right| \left|\langle \tfrac{3}{2} || \tfrac{1}{2} \rangle\right| \cdot \cos\phi_{31}, \tag{17}$$

where the cosine is either ± 1
(i. e. ϕ_{31} is the relative phase of the two matrix elements,
= 0 or 180 deg for a given resonance).

This discussion has been related to an example with only one resonant state; in this case, determinations of ρ at two different production angles were necessary. If two interfering resonances occur, ρ must be determined at eight production angles in (16a) and (16b) for parity determination, in order to untangle individual transitions. If one assumes a model of the resonance phases (with the sign undetermined), it turns out that (16c) could be resolved by only six production angle measurements to obtain the relative magnitudes of different helicity transitions. The situation is clearly complicated, but within the realm of current possibility.

It should be mentioned that recent analysis[6] of $\gamma N \rightarrow \pi N$ indicates that in the c. m. energy region 1450 to 1800 MeV, transitions from initial total helicity 1/2 are quite small compared with initial total helicity 3/2 transitions. This halves the number of different production angle measurements needed to perform the analysis as described above, simply by halving the number of significant transitions.

Summarizing, we find that the following types of measurements are relevant:

(a) Unpolarized production determines relative magnitudes of transitions to a given final state.

(b) Linear polarized production determines relative signs of such pairs of transitions.

(c) Parity of a resonance can be determined by an unpolarized production experiment, but possibly can be measured more clearly from the difference of the two circularly polarized reactions.

All these quantities require measurements of several production angles (which is no problem in bubble chamber experiments).

This situation is further complicated by probably large contributions from one-pion exchange. No further considerations can proceed without an understanding of these effects, which we briefly discuss in the next section (though no resolution of the problem is presented here), and which will become more apparent from the examples in Sec. V.

IV. MODELS OF THE REACTION $\gamma N \rightarrow \pi\Delta$

The charge mode of $\gamma N \rightarrow \pi\Delta$ that suffers least from large experimental backgrounds due to competing processes is the mode $\gamma p \rightarrow \pi^+\pi^- p$, which is complicated by interference of the one-pion-exchange (OPE) process with s-channel resonance amplitudes. In the brief literature on this reaction, there does not seem to be any unanimity on what constitutes a reasonable model for it. One group[7] achieves a fit to the data with no resonances, but with a drastically modified gauge-invariant version[8] of OPE. On the other hand, the Cambridge Bubble Chamber Group[9] includes only s-channel resonances to achieve a reasonable fit. (In their analysis, the assumption of a 50% inelasticity for the $D_{3/2}$ (1525) resonance and the experimental $D_{3/2}$ (1525) cross section in $\gamma p \rightarrow (\pi^0 p) + (\pi^+ n)$ leads to a $D_{3/2}$ cross section of 60 μb in $\gamma p \rightarrow \pi\Delta$; this already accounts for most of the observed $d\sigma$.)

A desirable program at this point would be to fit (more statistically significant) additional data with a combination of baryon resonances <u>and</u> OPE.[10]

It is our opinion that the Stichel-Scholz calculation places too great a significance on the modifications associated with gauge-invariant one-pion exchange. In particular, an important contributor in their scheme is the Δ-exchange graph, which one might expect to be strongly suppressed because the Δ is so far off its mass shell in the physical region. We expect that OPE will account for at most half of the observed amplitudes, and the reaction will indeed be useful for obtaining information on baryon resonance parameters (see Section V).

The use of a linearly polarized beam makes possible a closer scrutiny of any model of OPE for the following reason. The basic one-pion-exchange diagram is proportional to $\vec{\epsilon} \cdot q_{\pi}$, which can be made to vanish by choosing $\vec{\epsilon}$ perpendicular to the reaction plane ($\Phi = 90$ deg); in gauge-invariant models such as that of Ref. 8, other large corrections to the pion-exchange graph also vanish for $\Phi = 90$ deg. (This is not true, however, for the contact graph in the Stichel-Scholz model.) A comparison of $\Phi = 0$ deg and $\Phi = 90$ deg would thus provide an improved estimate of the relative importance of OPE + gauge-invariance-required terms and baryon resonance amplitudes.

V. SOME RESULTS FROM A SIMPLE MODEL CALCULATION

In this final section, we illustrate by explicit examples how various s-channel partial-wave amplitudes and their different possible (multipole or helicity) excitation modes will manifest themselves in the production and decay angular distributions of the Δ isobar if OPE is present simultaneously. These examples might help to decide which type of polarization of the photons would be preferred in an experiment. They also show the expected size and rapidity of variation of the density matrix elements as a function of production angle Θ. From this one can estimate over how large intervals in $\cos\Theta$ the decay distributions may be averaged without losing essential information, and how many events will be needed.

We assume that in a practical experiment the polarization of the initial and final nucleons would not be observed. This leaves the production differential cross section $d\sigma/d\Omega$ (production) $\propto \mathrm{Tr}\,\rho$ to be measured, together with five independent combinations[11] of the helicity density matrix elements $\rho_{\Lambda\Lambda'}$, which, according to (11), completely describe the decay angular distribution of the Δ:

$$\rho_{33} + \rho_{-3-3}, \qquad \mathrm{Re}(\rho_{31} - \rho_{-3-1}), \qquad \mathrm{Re}(\rho_{3-1} + \rho_{-31}),$$
$$\mathrm{Im}(\rho_{31} + \rho_{-3-1}), \qquad \mathrm{Im}(\rho_{3-1} - \rho_{-31}).$$

Note that, as always in this paper, ρ is an unnormalized density matrix.[12] The above quantities are functions of $\cos\Theta$ and can simply be obtained, for example, from the experimental decay angular distributions in relatively small intervals of $\cos\Theta$ by calculation of the moments.

Our model consists in assuming that the transition amplitude is a sum of a relatively small number of s-channel resonant and nonresonant partial-wave amplitudes, plus OPE. The partial-wave amplitudes are characterized by J^P, by the magnitude $\lambda_i = |\lambda-\mu|$ of the initial-state total helicity, and by the orbital angular momentum ℓ_f in the final $\pi\Delta$ state.[13] Here $\lambda_i = 1/2,\ 3/2$, and $\ell_f = J \mp 3/2,\ J \pm 1/2$ [for $P = (-)^{J \mp 1/2}$]. The production amplitude may then be written in the form[14]

$$T_{\Lambda\mu}^{(\lambda)}(s,\Theta) = \left[\frac{(8\pi)^3 s}{k_\gamma q_\pi}\right]^{1/2} \sum_{J,\ell_f} \sqrt{J+1/2}\ \langle \ell_f | T^J(s) | \lambda\mu\rangle$$
$$\times \sum_{m=-3/2}^{3/2} C(\ell_f, \tfrac{3}{2}, J;\ \mu-\lambda-m, m)\ Y_{\ell_f}^{\mu-\lambda-m}(\Theta, 0)\, d_{m\Lambda}^{(3/2)}(\Theta) \tag{18}$$
$$+ B_{\Lambda\mu}^{(\lambda)}(s,\Theta),$$

with the normalization defined by (4). The connection with the S matrix is given by $T^J(s) = S^J(s)/2i$. The parity relations are easily seen to be

$$\langle \ell_f | T^J | -\lambda-\mu\rangle = (-)^{J+1/2-\ell_f}\ \langle \ell_f | T^J | \lambda\mu\rangle. \tag{19}$$

We also write $\langle \ell_f | T^J | \lambda_i\rangle$ instead of $\langle \ell_f | T^J | \lambda\mu\rangle$ for $\lambda-\mu>0$. The OPE helicity amplitudes $B_{\Lambda\mu}^{(\lambda)}$ are readily calculated, with the result

$$B_{\Lambda\mu}^{(\lambda)}(s,\Theta) = eg^* \left[\frac{(m_N+E_N)(m_\Delta+E_\Delta)}{4m_\pi^2}\right]^{1/2} \frac{\lambda\beta_\pi \sin\Theta}{1-\beta_\pi\cos\Theta}\ H_{\Lambda\mu}(\Theta), \tag{20}$$

where

$$H_{\pm 3/2\ 1/2}(\Theta) = -(1 \mp \delta)\ \sin\Theta \begin{Bmatrix}\cos\\ \sin\end{Bmatrix}\frac{\Theta}{2},$$
$$H_{\pm 1/2\ 1/2}(\Theta) = \sqrt{\frac{1}{3}}\left[(1\pm\delta)\ \sin\Theta \begin{Bmatrix}\sin\\ \cos\end{Bmatrix}\frac{\Theta}{2} \pm 2(1\mp\delta)\gamma_\Delta\left(\frac{\beta_\Delta}{\beta_N} - \cos\Theta\right)\begin{Bmatrix}\cos\\ \sin\end{Bmatrix}\frac{\Theta}{2}\right], \tag{21}$$
$$H_{\Lambda,-1/2}(\Theta) = (-)^{\Lambda+1/2}\ H_{-\Lambda,1/2}(\Theta).$$

Here k_γ and q_π are the momenta, E_N and E_Δ the energies, and β_π, β_Δ, and β_N the velocities of the indicated particles, all in the c.m. system; $\delta = \beta_N\beta_\Delta\gamma_N\gamma_\Delta/\left((\gamma_N+1)(\gamma_\Delta+1)\right)$ and $\gamma = (1-\beta^2)^{-1/2}$. Further, Λ, λ, and μ are the helicities of Δ, photon, and incident N. Finally, $e \approx \pm\sqrt{4\pi/137}$ (for $\pi^\pm$), and the $\Delta N\pi$ vertex has been written as $(g^*/m_\pi)\, \bar{u}_\alpha(p')\, u(p)\, p_\alpha$.[15]

For the OPE amplitudes the radiation gauge in the c.m. system has been taken.[10] Any corrections to this might be thought of as being already represented in the phenomenological sum over partial waves in (18).

In the examples that follow, the six "observable" combinations of the helicity density matrix elements $\rho_{\Lambda\Lambda'}$ are shown for different assumed sets of amplitudes $\langle \ell_f | T^J | \lambda_i \rangle$. In absence of reliable knowledge on these amplitudes, the phases were taken to be equal (modulo 180 deg) to the elastic πN scattering phases[16] at the same total c.m. energy, and relative magnitudes were estimated by using the inelasticities from the πN phase-shift analysis[16] together with the known information[17] on the branching ratios $\sigma^{JP}_{\Delta\pi}/\sigma^{JP}_{inel}$ into the $\pi\Delta$ channel. This is of course only a rough first guess at what amplitudes might actually be present.

In Figs. 2 through 5, $W(\cos\Theta)$ is the production angular distribution for unpolarized (or circularly polarized) photons, normalized to

$$\int_{-1}^{1} W(\cos\Theta)\, d\cos\Theta = 1.$$

Accordingly, the $\rho_{\Lambda\Lambda'}$ are equal to the normalized helicity density matrix elements multiplied by $W(\cos\Theta)$. Also $W^{(a)}(\cos\Theta) = \mathrm{Tr}\,\rho^{(a)}$, so that for linearly polarized photons the production angular distribution is given by $W \pm W^{(a)}$ for $\Phi = 0$ deg and $\Phi = 90$ deg, respectively.

The first example (Fig. 2) shows results for a superposition of $J^P = 3/2^-$, $5/2^+$ and $7/2^+$ amplitudes at $E_{cm} = 1680$ MeV, with 50% OPE added.[18] Also shown is the effect of a change of parity in the 5/2 amplitude, as well as the results for $3/2^-$, $5/2^+$, $5/2^-$, and $7/2^+$ amplitudes superposed, and with further addition of small $1/2^-$ and $1/2^+$ amplitudes. It appears that changing the parity of the 5/2 amplitude has a strong effect already on the "unpolarized" information. However, adding $1/2^-$ or $1/2^+$ waves shows very little effect there; it has some effect on the $\mathrm{Im}\rho_{\Lambda\Lambda'}$ (which are measurable by using circularly polarized photons), but the

Fig. 2. The observables (production angular distributions and helicity density matrix elements) for E_{cm} = 1680 MeV, assuming the following set of amplitudes. (Note 23):

——— $(3/2^-, 3/2; 0.23, 126\ \text{deg}) + (5/2^+, 3/2; 0.27, 130\ \text{deg})$ $+ (7/2^+, 3/2; 0.07, 201\ \text{deg})$ + 50% OPE

—×— same as ———, with $5/2^+$ replaced by $5/2^-$

—+— same as ———, added $(5/2^-, 3/2; 0.18, 303\ \text{deg})$

—□— same as —+—, added $(1/2^-, 1/2; 0.16, 291\ \text{deg})$

—△— same as —□—, added $(1/2^+, 1/2; 0.20, 83\ \text{deg})$

For the normalization of the angular distributions and the $\rho_{\Lambda\Lambda'}$, see the text.

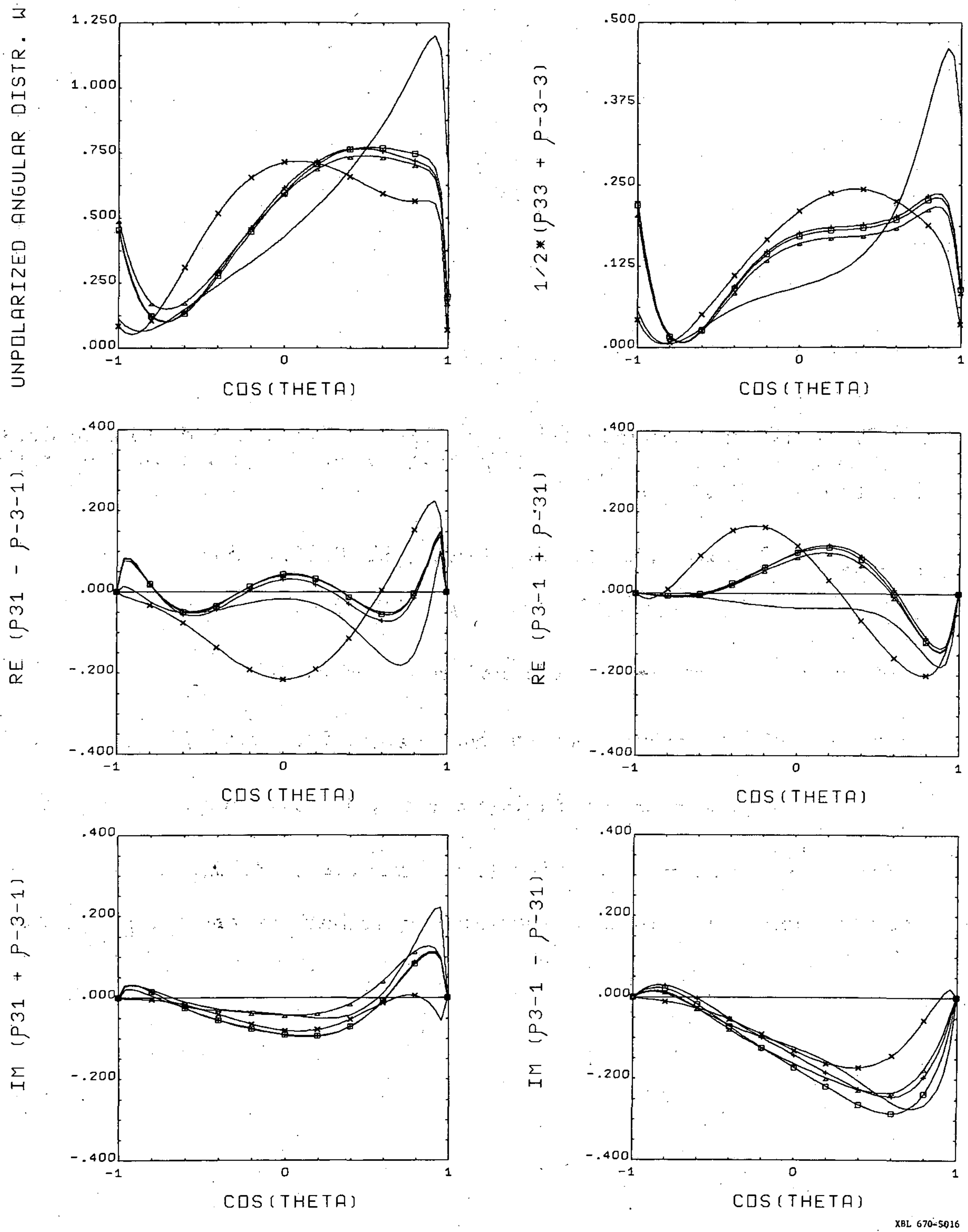
UNPOLARIZED ANGULAR DISTR. W
1.250
1.000
.750
.500
.250
.000
-1
0
1
COS(THETA)
1/2*(ρ33 + ρ-3-3)
.500
.375
.250
.125
.000
COS(THETA)
RE (ρ31 - ρ-3-1)
.400
.200
.000
-.200
-.400
COS(THETA)
RE (ρ3-1 + ρ-31)
COS(THETA)
IM (ρ31 + ρ-3-1)
COS(THETA)
IM (ρ3-1 - ρ-31)
COS(THETA)
XBL 670-5016

Fig. 2a

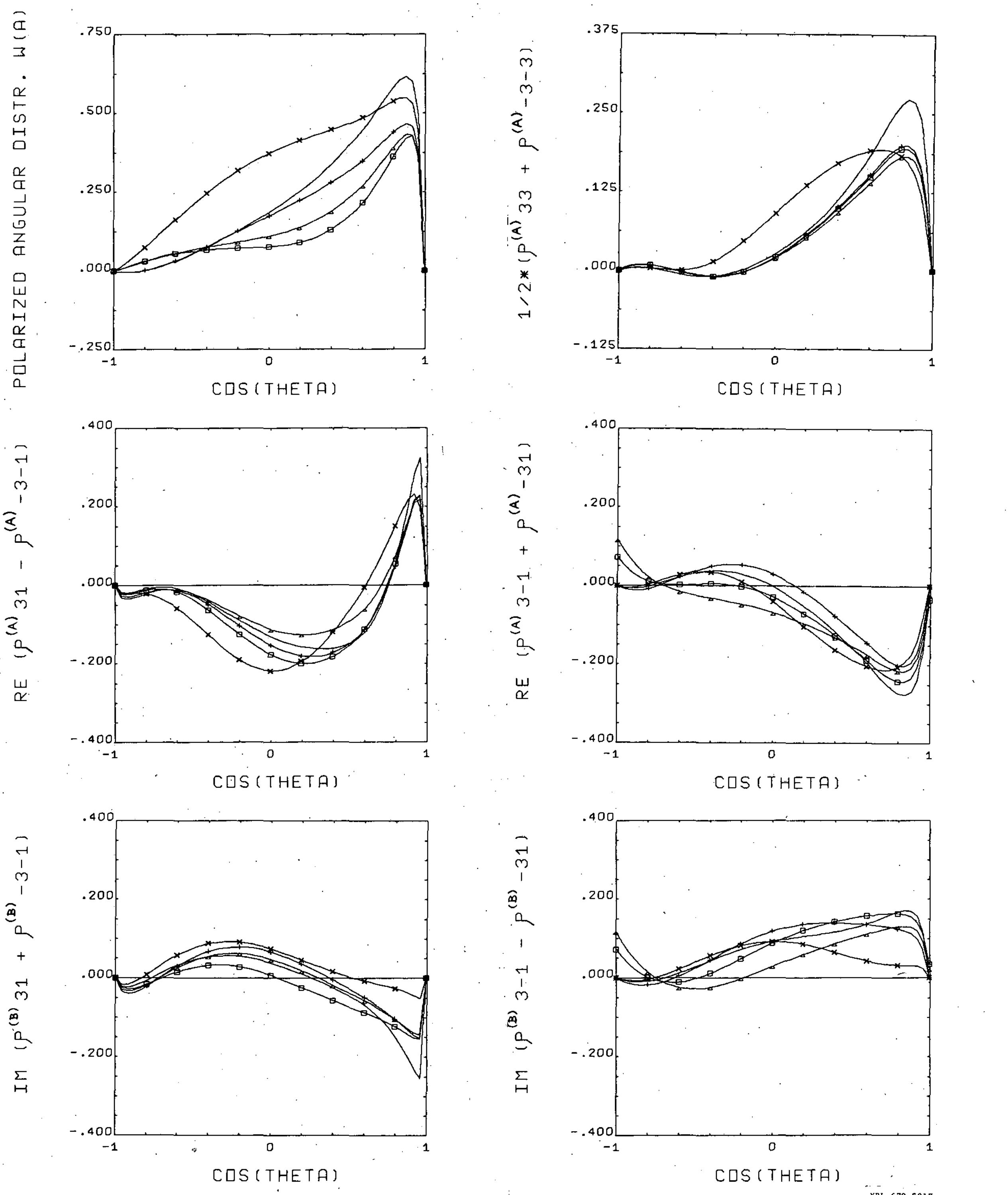
POLARIZED ANGULAR DISTR. W(A)
.750
.500
.250
.000
-.250
-1
0
1
COS(THETA)
1/2*(ρ(A)33 + ρ(A)-3-3)
.375
.250
.125
.000
-.125
-1
0
1
COS(THETA)
RE (ρ(A)31 - ρ(A)-3-1)
.400
.200
.000
-.200
-.400
-1
0
1
COS(THETA)
RE (ρ(A)3-1 + ρ(A)-31)
.400
.200
.000
-.200
-.400
-1
0
1
COS(THETA)
IM (ρ(B)31 + ρ(B)-3-1)
.400
.200
.000
-.200
-.400
-1
0
1
COS(THETA)
IM (ρ(B)3-1 - ρ(B)-31)
.400
.200
.000
-.200
-.400
-1
0
1
COS(THETA)
XBL 670-5017

Fig. 2b

Fig. 3. The observables for E_{cm} = 1680 MeV, with varying helicity λ_i and multipole of the $5/2^+$ resonance (Note 23):

——— $(3/2^-, 3/2; 0.23, 126\text{ deg}) + (5/2^+, 3/2; 0.27, 130\text{ deg}) + (7/2^+, 3/2; 0.07, 201\text{ deg}) + 50\%$ OPE

—×— same as ———, with $\lambda_i = 3/2$ replaced by $\lambda_i = 1/2$ for the $5/2^+$

—+— same as ———, with $\lambda_i = 3/2$ replaced by E2 for the $5/2^+$

—⊟— same as ———, with $\lambda_i = 3/2$ replaced by M3 for the $5/2^+$

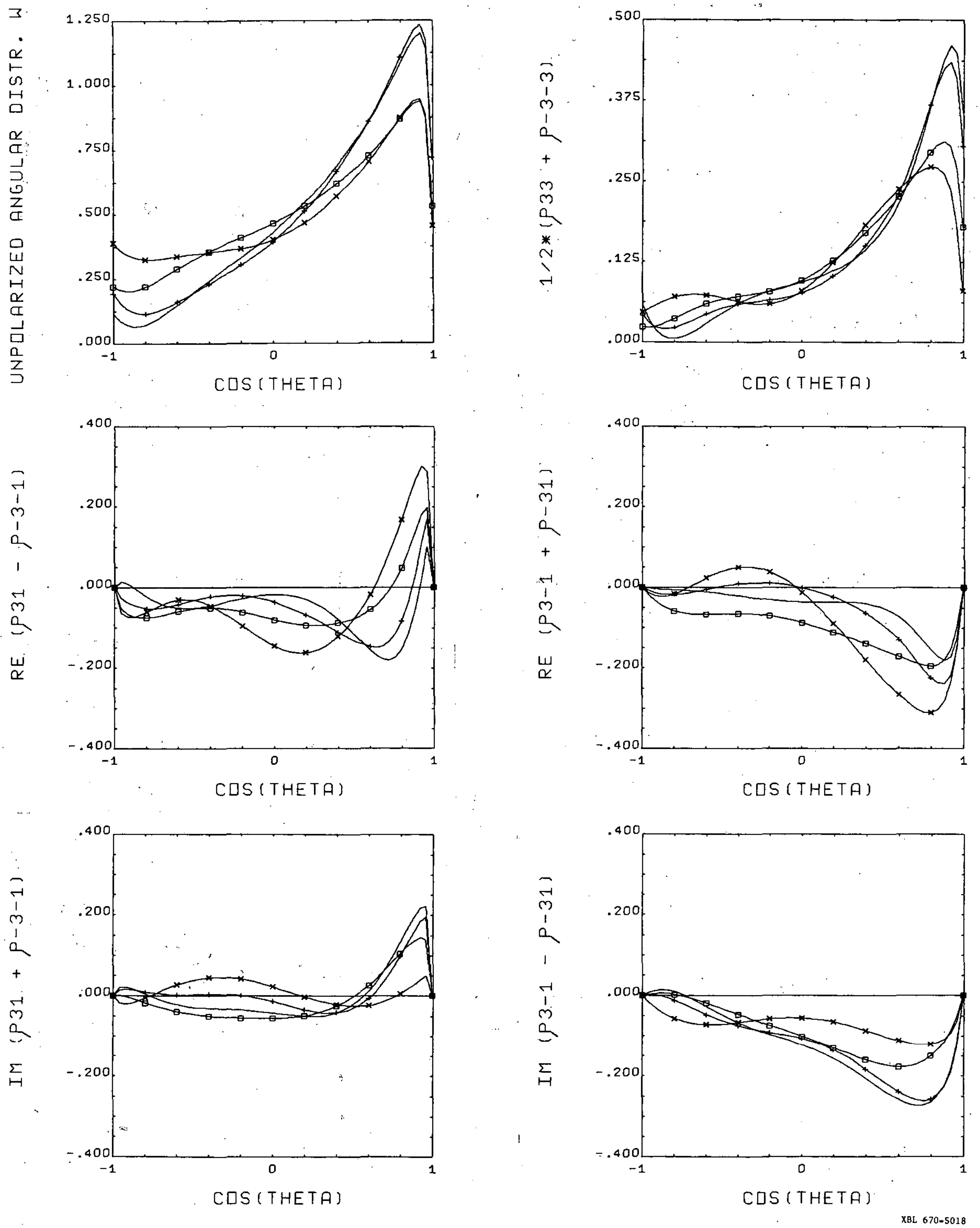
UNPOLARIZED ANGULAR DISTR. W
1.250
1.000
.750
.500
.250
.000
-1
0
1
COS(THETA)
1/2*(ρ33 + ρ-3-3)
.500
.375
.250
.125
.000
COS(THETA)
RE (ρ31 - ρ-3-1)
.400
.200
.000
-.200
-.400
COS(THETA)
RE (ρ3-1 + ρ-31)
COS(THETA)
IM (ρ31 + ρ-3-1)
COS(THETA)
IM (ρ3-1 - ρ-31)
COS(THETA)
XBL 670-5018

Fig. 3a

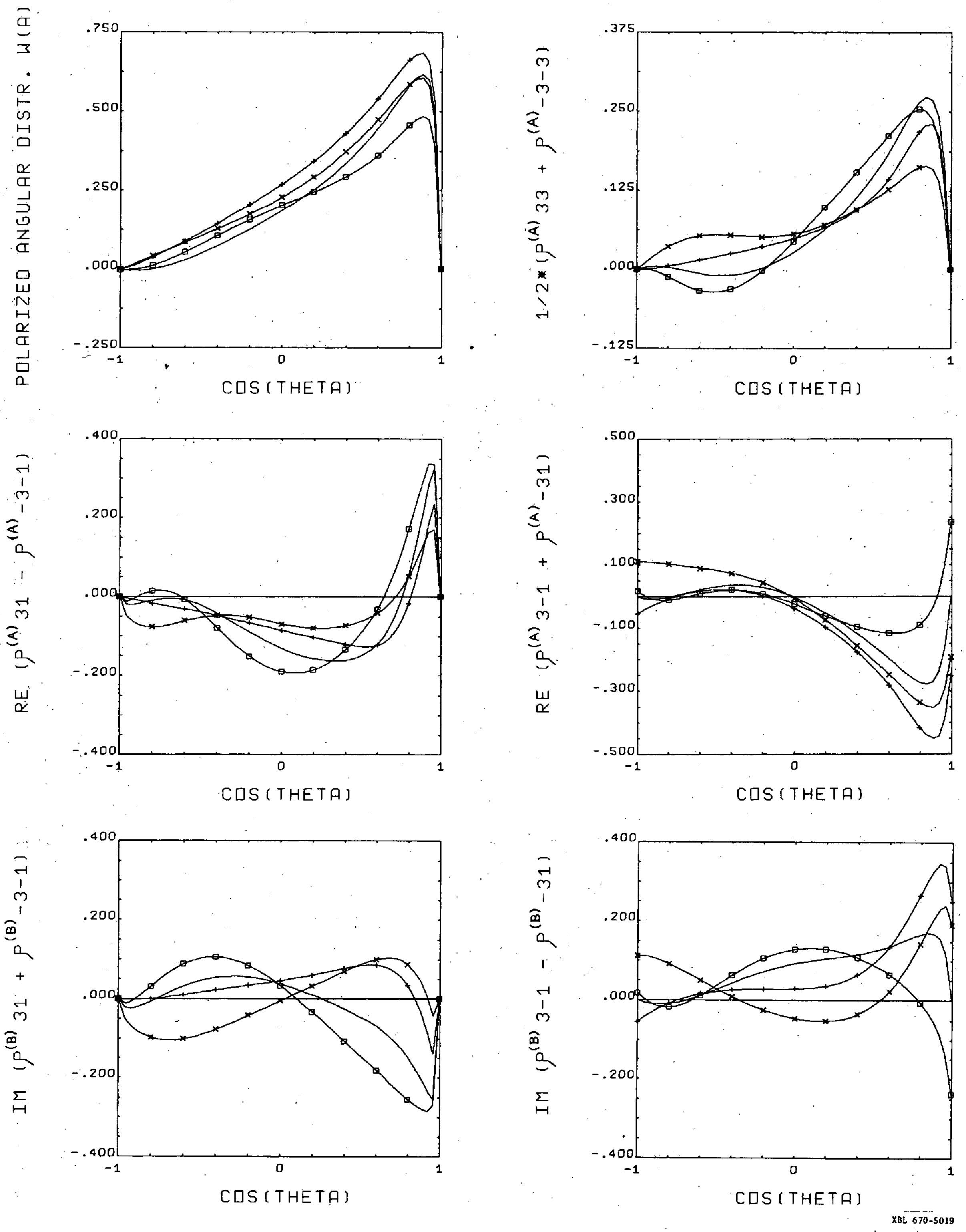
POLARIZED ANGULAR DISTR. W(A)
COS(THETA)
1/2*(ρ(A) 33 + ρ(A) -3-3)
RE (ρ(A) 31 - ρ(A) -3-1)
RE (ρ(A) 3-1 + ρ(A) -31)
IM (ρ(B) 31 + ρ(B) -3-1)
IM (ρ(B) 3-1 - ρ(B) -31)
XBL 670-5019

Fig. 3b

Fig. 4. The observables for E_{cm} = 1680 MeV with varying contributions of OPE.

——— $(1/2^+,\ 1/2;\ 0.20,\ 83\ \text{deg}) + (1/2^-,\ 1/2;\ 0.16,\ 291\ \text{deg})$
$+ (3/2^-,\ 3/2;\ 0.23,\ 126\ \text{deg}) + (5/2^+,\ 3/2;\ 0.27, 130\ \text{deg})$
$+ (5/2^-,\ 3/2;\ 0.18,\ 303\ \text{deg}) + (7/2^+,\ 3/2;\ 0.07,\ 201\ \text{deg})$ + 0% OPE

—×— same with 20% OPE

—+— same with 40% OPE

—□— same with 70% OPE

—△— pure OPE

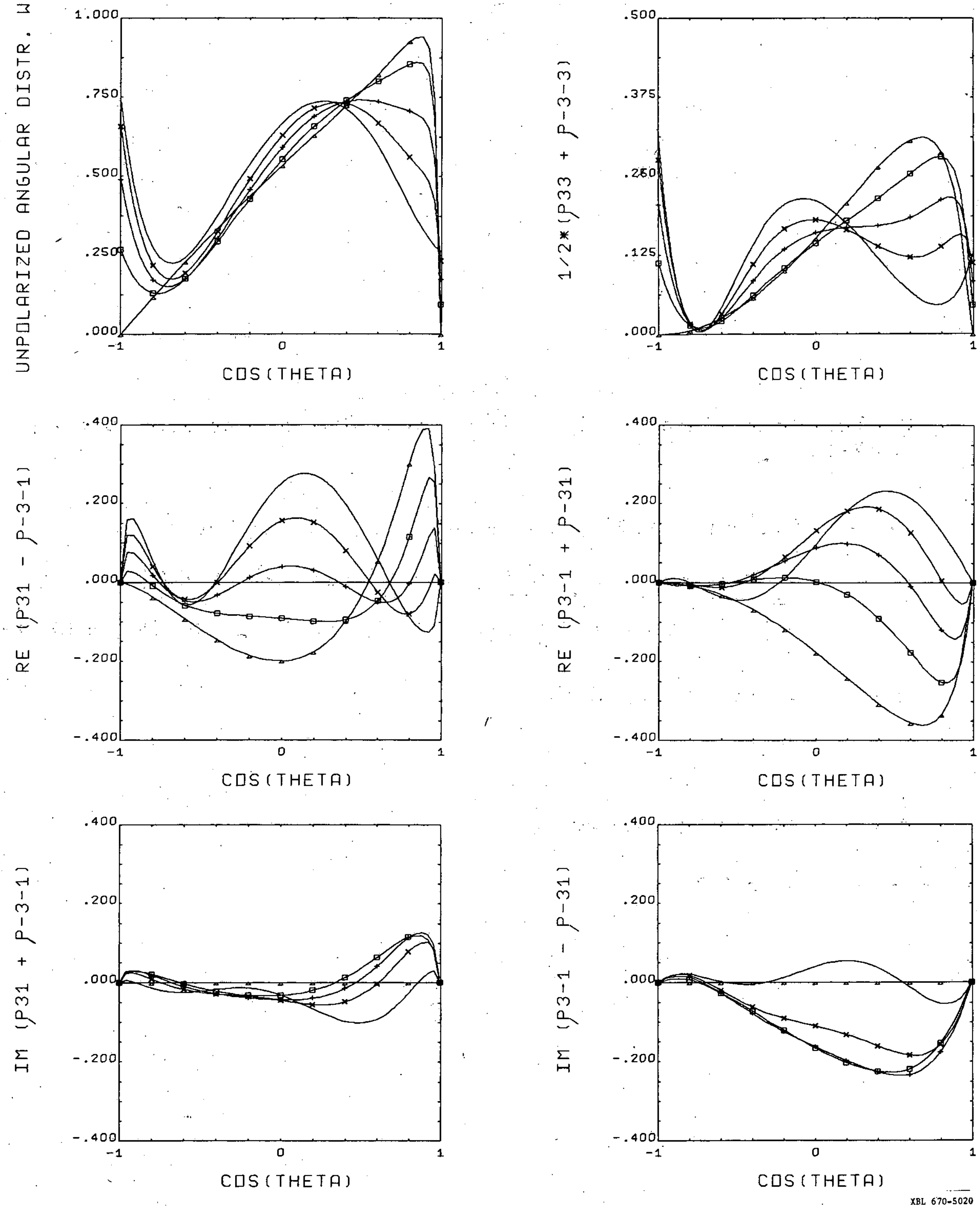
UNPOLARIZED ANGULAR DISTR. W
1/2*(ρ33 + ρ-3-3)
RE (ρ31 - ρ-3-1)
RE (ρ3-1 + ρ-31)
IM (ρ31 + ρ-3-1)
IM (ρ3-1 - ρ-31)
COS(THETA)
1.000
.750
.500
.250
.000
.375
.125
.400
.200
-.200
-.400
-1
0
1
XBL 670-5020

Fig. 4a

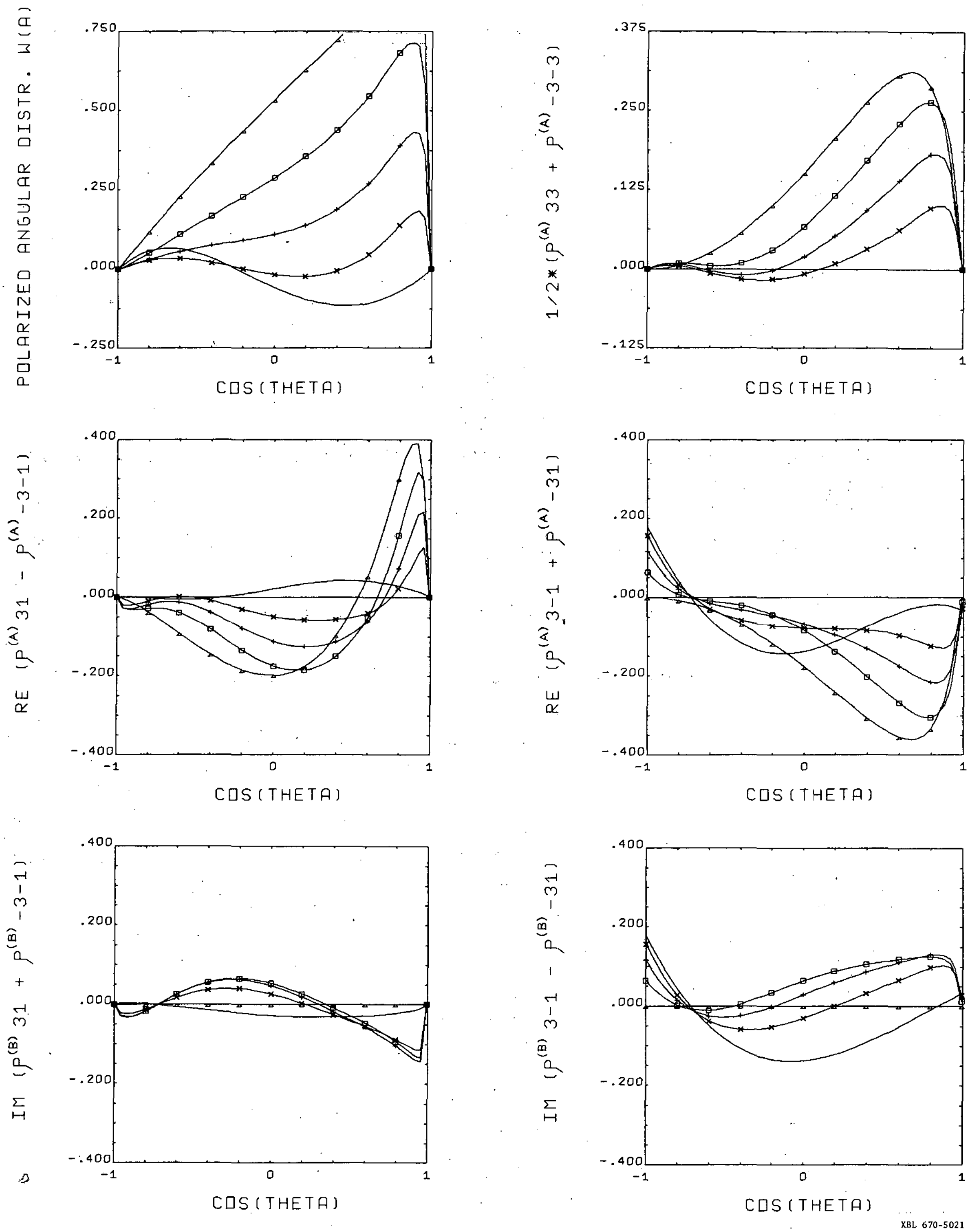
POLARIZED ANGULAR DISTR. W(A)
.750
.500
.250
.000
-.250
-1
0
1
COS(THETA)
1/2*(ρ(A) 33 + ρ(A) -3-3)
.375
.250
.125
.000
-.125
-1
0
1
COS(THETA)
RE (ρ(A) 31 - ρ(A) -3-1)
.400
.200
.000
-.200
-.400
-1
0
1
COS(THETA)
RE (ρ(A) 3-1 + ρ(A) -31)
.400
.200
.000
-.200
-.400
-1
0
1
COS(THETA)
IM (ρ(B) 31 + ρ(B) -3-1)
.400
.200
.000
-.200
-.400
-1
0
1
COS(THETA)
IM (ρ(B) 3-1 - ρ(B) -31)
.400
.200
.000
-.200
-.400
-1
0
1
COS(THETA)
XBL 670-5021

Fig. 4b

Fig. 5. The observables for E_{cm} = 1450 MeV, assuming various sets of amplitudes (Note 23):

——— $(3/2^-, 3/2; 0.49, 103\ \text{deg}) + (5/2^-, 3/2; 0.16, 213\text{deg})$ + 50% OPE

—×— same as ———, added $(1/2^+, 1/2; 0.19, 113\ \text{deg})$

—+— same as —×—, added $(1/2^-, 1/2; 0.11, 332\ \text{deg})$

—⊟— same as —+—, with $\lambda_i = 3/2$ replaced by E1 for the $3/2^-$.

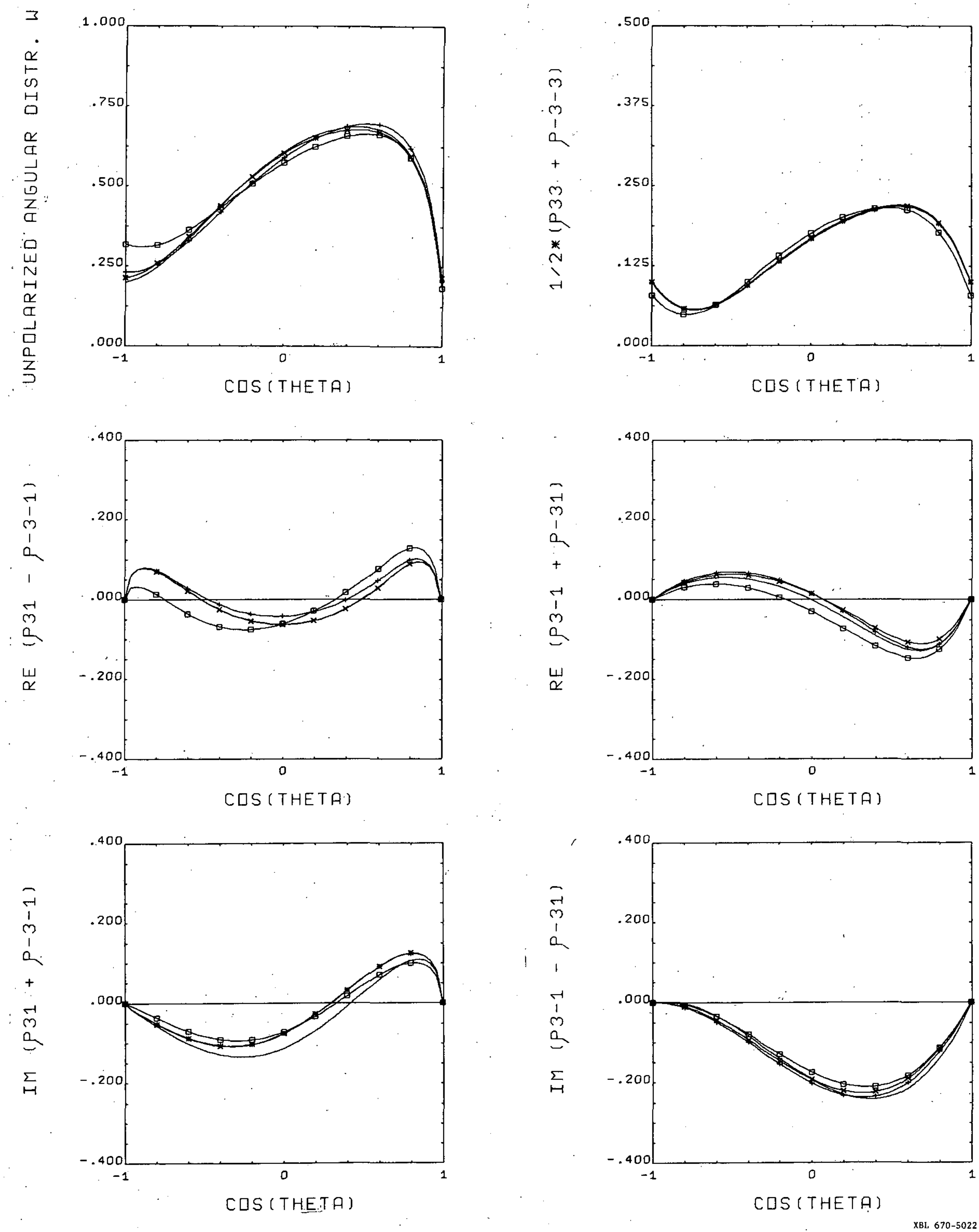
UNPOLARIZED ANGULAR DISTR. W
1.000
.750
.500
.250
.000
-1
0
1
COS(THETA)
1/2*(ρ33 + ρ-3-3)
.500
.375
.250
.125
.000
RE (ρ31 - ρ-3-1)
.400
.200
.000
-.200
-.400
RE (ρ3-1 + ρ-31)
IM (ρ31 + ρ-3-1)
IM (ρ3-1 - ρ-31)
XBL 670-5022

Fig. 5a

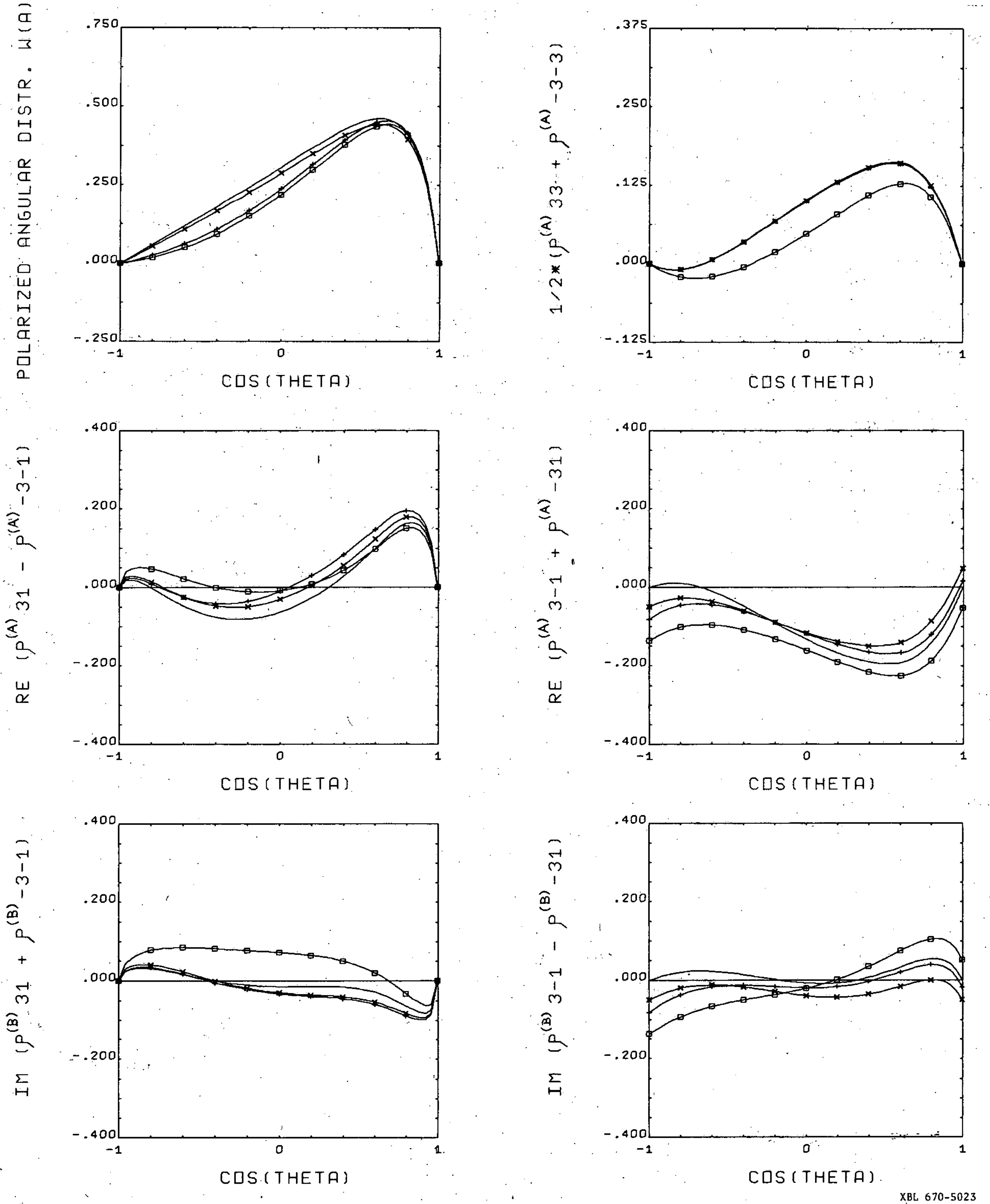
POLARIZED ANGULAR DISTR. W(A)
.750
.500
.250
.000
-.250
-1
0
1
COS(THETA)
1/2*(ρ(A) 33 + ρ(A) -3-3)
.375
.250
.125
.000
-.125
RE (ρ(A) 31 - ρ(A) -3-1)
.400
.200
.000
-.200
-.400
RE (ρ(A) 3-1 + ρ(A) -31)
IM (ρ(B) 31 + ρ(B) -3-1)
IM (ρ(B) 3-1 - ρ(B) -31)
XBL 670-5023

Fig. 5b

strongest effect is in $W^{(a)}$ and in some of the other $\rho^{(a)}_{\Lambda\Lambda'}$ and $\rho^{(b)}_{\Lambda\Lambda'}$, measurable with linearly polarized photons only.

A major aim of an experiment on $\gamma p \rightarrow \pi\Delta$ would be to study the electromagnetic properties of resonances, that is, the characteristics of the electromagnetic excitation process of the resonant partial waves. Therefore in the next example (Fig. 3) we compare different excitation modes of the $5/2^+$ resonance at $E_{cm} = 1680$ MeV, assuming the additional presence of $3/2^-$ and $7/2^+$ partial waves and of OPE. One sees that under these circumstances, dis crimination between helicities $\lambda_i = 1/2$ and $\lambda_i = 3/2$ would be possible even with unpolarized photons; for example, $W(\cos\Theta)$ in the backward direction is sensitive to this. Alternatively, the excitation may be characterized by multipole amplitudes[19] E2 or M3, but for distinguishing these linear polarization would clearly be advantageous.

Since OPE contributes considerably[7] in the charge mode $\gamma p \rightarrow \pi^- \Delta^{++}$, which is most easily accessible experimentally, in Fig. 4 the consequences of varying the amount of OPE are shown, again at 1680 MeV with $1/2^{\pm}$, $3/2^-$, $5/2^{\pm}$, and $7/2^+$ partial waves added. Note that OPE alone leads to a purely real density matrix. There is nevertheless an effect on Im ρ from OPE through interference but it is much less pronounced than in Re ρ. For pure OPE, also $\rho^{(a)} \equiv \rho^{(\pm 1)}$ due to the $(\epsilon . q)$ coupling.

Finally, we study the possible situation at $E_{cm} = 1450$ MeV, where the dominant contributions are expected to come from $3/2^-$ and $5/2^-$ partial waves plus OPE. Of particular interest[20,21] is the effect of adding contributions of $1/2^+$ and $1/2^-$ amplitudes. It appears (Fig. 5) that it certainly would be very hard to detect small $1/2^{\pm}$ waves from the "unpolarized" data alone.[22] There is some sensitivity to these partial waves in Im $\rho^{(\pm 1)}$, measurable with circular polarization; but the additional information appearing in the data from linear polarization, $\rho^{(a)}$ and $\rho^{(b)}$, would probably also be needed. On the other hand, the unpolarized data are sensitive to $\lambda_i = 3/2$ vs E1 excitation of the dominant $3/2^-$ partial wave.

In conclusion, it appears that measurements of $\pi\Delta$ photoproduction could indeed be a useful and sensitive tool to further investigate photoproduction in the baryon resonance region. Polarizing the photon beam would considerably amplify the amount of information that can be obtained, and in fact is crucial for most of the interesting aspects of such experiments.

ACKNOWLEDGMENTS

We thank Dr. Arthur H. Rosenfeld, Dr. Haim Harari, and Dr. Robert Thews for useful discussions, and Mr. Dennis Sivers for help with computer programming.

This work was done under auspices of the U. S. Atomic Energy Commission.

FOOTNOTES AND REFERENCES

*Present address: CERN, Geneva, Switzerland.

1. The reader will find discussions presented on other related reactions in the recent literature, such as Proceedings of the International Symposium on Electron and Photon Interactions at High Energies, Springer Tracts in Modern Physics, Vol. 39 (1965).
2. R. H. Milburn, Phys. Rev. Letters 10, 75 (1963);
F. R. Arutyunian and V. A. Tumanian, Phys. Letters 4, 176 (1963);
J. J. Murray and P. R. Klein, SLAC-TN-67-19 (1967), unpublished.
3. K. Gottfried and J. D. Jackson, Nuovo Cimento 33, 309 (1964).
4. M. Jacob and G. C. Wick, Ann. Phys. 7, 404 (1959).
5. The Clebsch-Gordan and Racah coefficients are defined in M. E. Rose, Elementary Theory of Angular Momentum (John Wiley and Sons, Inc., New York, 1957).
6. R. L. Walker, Cal. Tech. Synchrotron Report (unpublished); S. D. Ecklund and R. L. Walker, Phys. Rev. 159, 1195 (1967).
7. German Bubble Chamber Collaboration, Phys. Letters 23, 707 (1966).
8. P. Stichel and M. Scholz, Nuovo Cimento 34, 1381 (1964). See also M. P. Locher and W. Sandhaus, Z. Physik 195, 461 (1966);
K. Böckmann, W. Sandhaus, and H. Wessel, Z. Physik 202, 477 (1967).
9. Cambridge Bubble Chamber Group, Production of the $N^*(1238)$ Nucleon Isobar by Photon of Energy up to 6 BeV, preprint, June 1967, submitted to Phys. Rev.
10. Pure one-pion exchange might in a formal way be "modified", à la Drell replacing $\epsilon \cdot q$ by $\epsilon \cdot (q - p \frac{k \cdot q}{k \cdot p})$, which is gauge invariant, and equal to $\epsilon \cdot q$ with the radiation gauge in the c.m. system. (Here k, p, and q are the four-momenta of photon, incident proton, and outgoing pion (π_1), respectively.) Then, $\sum_{\Lambda} |OPE|^2$ would still be proportional to $q^2 \sin^2\Theta$; one can check that this graph contributes $\sigma_{tot} \approx 20\ \mu b$ in $\gamma p \to \pi\Delta$.
11. The reaction $\gamma p \to \pi\Delta$, in a definite charge mode, is in general described by $2 \times 2 \times 4 = 16$ helicity amplitudes. Parity conservation halves the number of independent amplitudes. Since an overall phase is arbitrary, there are 15 independent real functions of Θ and the energy which completely specify the transition matrix. The experiment discussed here is therefore far from being "complete."

12. The $\rho_{\Lambda\Lambda'}$ are of more basic experimental interest than is the <u>normalized</u> density matrix. It is the $\rho_{\Lambda\Lambda'}$ which are observed most directly by measuring the decay distributions. They also have a simpler $\cos\Theta$ dependence, obeying a "maximum complexity theorem" similar to that for unpolarized angular distributions.

13. In the energy region under consideration, angular momentum barriers are generally expected to suppress the $\ell_f = J+1/2$, $J+3/2$ amplitudes relative to the amplitudes for the lower ℓ_f. This is the reason why we label the amplitudes by ℓ_f instead of, say, the helicity Λ in the final state.

14. This is preferred for numerical application over the Jacob-Wick expansion (Ref. 4), since it does not involve the $d^{(J)}_{MM'}$ for arbitrary J. The numerical factors can easily be checked by equating (18) with the usual expansion (Ref. 4) for, say, $\Theta = 0$.

15. This leads to an expression for the width of the Δ,

$$\Gamma_\Delta = (g^{*2}/4\pi)\, q^3_{decay}\, \frac{(m_\Delta + m_N)^2 - m_\pi^2}{6m_\Delta^2\, m_\pi^2} ,$$

where q_{decay} is the momentum of the decay pion (π_2) in the Δ rest frame.

16. P. Bareyre, C. Bricman, and G. Villet, preprint (Aug. 1967), submitted to Phys. Rev.

17. A. H. Rosenfeld, N. Barash-Schmidt, A. Barbaro-Galtieri, W. J. Podolsky, L. R. Price, M. Roos, P. Söding, W. J. Willis, and C. G. Wohl, UCRL-8030, Sept. 1967, unpublished.

18. What is meant is that each--the OPE amplitude and the explicit partial-wave sum--taken alone would lead to identical total cross sections. (Actually, the cross section for the sum is 90% of the sum of the individual cross sections, showing that there is some though little destructive interference.)

19. The multipole amplitudes are linear combinations of the helicity amplitudes. They are easily found from the expansion of the corresponding states

$$|JM; \lambda\mu\rangle = \sum_{j^\pi} \left[\frac{2j+1}{2(2J+1)}\right]^{1/2} (-\lambda)^p \; C(j \tfrac{1}{2} J; \lambda, -\mu) \,|\, JM; j^\pi \tfrac{1}{2}\rangle$$

where the total angular momentum and parity of the photon are j and $\pi = (-)^{j+p}$, respectively, with $p = 0$ (electric 2^j pole) or $p = 1$ (magnetic 2^j pole).

20. R. G. Moorhouse, Phys. Rev. Letters 16, 772 (1966)
21. A. Donnachie, Phys. Letters 24B, 420 (1967).
22. Note that a $J = 1/2$ partial wave does not contribute to ρ_{33} and ρ_{-3-3} at all, and to ρ_{31}, ρ_{3-1}, ρ_{-31}, ρ_{-3-1} only through interference with amplitudes having $J > 1/2$.
23. The notation used for the amplitudes $\langle \ell_f | T^J | \lambda_i \rangle$ is (J^P, helicity λ_i (or multipole); relative magnitude, phase angle). Generally, the lowest possible value of ℓ_f is always taken (Note 13). For the OPE contribution, see footnote 18.